This article was downloaded by: [Dmitriy Kupriyanov]
On: 07 October 2011, At: 10:27
Publisher: Taylor & Francis
Informa Ltd Registered in England and Wales Registered Number: 1072954 Registered office: Mortimer House, 37-41 Mortimer Street, London W1T 3JH, UK

Journal of Modern Optics
Publication details, including instructions for authors and subscription information:
http://www.tandfonline.com/loi/tmop20

Coherent backscattering under conditions of electromagnetically induced transparency

I.M. Sokolov [a b], D.V. Kupriyanov [a] & M.D. Havey [c]

[a] Department of Theoretical Physics, State Polytechnic University, St. Petersburg 195251, Russia

[b] Institute for Analytical Instrumentation, RAS, St. Petersburg 198103, Russia

[c] Department of Physics, Old Dominion University, Norfolk, VA 23529, USA

Available online: 11 Jul 2011

To cite this article: I.M. Sokolov, D.V. Kupriyanov & M.D. Havey (2011): Coherent backscattering under conditions of electromagnetically induced transparency, Journal of Modern Optics, DOI:10.1080/09500340.2011.594180

To link to this article: http://dx.doi.org/10.1080/09500340.2011.594180

PLEASE SCROLL DOWN FOR ARTICLE

Full terms and conditions of use: http://www.tandfonline.com/page/terms-and-conditions

This article may be used for research, teaching, and private study purposes. Any substantial or systematic reproduction, redistribution, reselling, loan, sub-licensing, systematic supply, or distribution in any form to anyone is expressly forbidden.

The publisher does not give any warranty express or implied or make any representation that the contents will be complete or accurate or up to date. The accuracy of any instructions, formulae, and drug doses should be independently verified with primary sources. The publisher shall not be liable for any loss, actions, claims, proceedings, demand, or costs or damages whatsoever or howsoever caused arising directly or indirectly in connection with or arising out of the use of this material.

Journal of Modern Optics
2011, 1–8, iFirst

Taylor & Francis
Taylor & Francis Group

Coherent backscattering under conditions of electromagnetically induced transparency

I.M. Sokolov[a,b], D.V. Kupriyanov[a] and M.D. Havey[c]*

[a]*Department of Theoretical Physics, State Polytechnic University, St. Petersburg 195251, Russia;* [b]*Institute for Analytical Instrumentation, RAS, St. Petersburg 198103, Russia;* [c]*Department of Physics, Old Dominion University, Norfolk, VA 23529, USA*

(*Received 27 February 2011; final version received 24 May 2011*)

We consider the influence of a resonant control field on weak localization of light in ultracold atomic ensembles. Both steady-state and pulsed light excitation are considered. We show that the presence of a control field essentially changes the type of interference effects that occur under conditions of multiple scattering. For example, for some scattering polarization channels the presence of a control field can cause destructive interference through which the enhancement factor, normally considered to be greater than one, becomes less than one.

Keywords: coherent backscattering; electromagnetically induced transparency; weak localization; antilocalization

Downloaded by [Dmitriy Kupriyanov] at 10:27 07 October 2011

1. Introduction

Interference effects under multiple light scattering in optically thick disordered media have been subject to intense investigation for almost three decades. Coherent backscattering (CBS), which is closely related to weak localization, is one of the striking examples of the types of effects that can occur. CBS manifests itself as an enhancement of the intensity of light scattered in the nearly backwards direction. Wave scattering in this direction along reciprocal, or time-reversed, multiple scattering paths preserves the relative phase, which results in constructive interference. The first detailed observations and analysis of this effect for light were made in [1–3] and by now CBS in solids and liquids has been investigated in detail [4–6].

Observation of CBS of light in atomic gases is complicated because atomic motion causes random phase shifts of scattering waves, which are different for reciprocal paths. For this reason, the weak localization has been observed only for a cold atomic ensemble. The first experiments on CBS in ultracold atomic samples prepared in a magneto-optical trap [7–9] showed that there is a range of interesting features of this phenomena compared with CBS observed earlier for solids and liquids [4–6]. These features, which have their origin in the atomic nature of the scatterers, could not be understood and quantitatively described by approaches developed previously for classical scatterers such as powders and suspensions.

Detailed treatments of CBS, taking into account the quantum nature of atomic scatterers, was developed by several groups [10–16]. In these papers, different aspects of weak localization were considered. In particular, it was shown that one can have a strong influence on the observed interferences by reinforcing those scattering channels that lead to interference and suppressing those that do not. Such desirable effects can be realised for example by polarization of atomic angular moments. By means of optical orientation effects it is possible to collect all atoms in one Zeeman sublevel, ensuring the fulfillment of optimal interference. Similar effects can be achieved by applying an auxiliary static magnetic field and tuning the frequency of the light in such a way that light would interact only with the desired Zeeman sublevel [17].

Experiment [17] has shown that a static external field influences the process of multiple scattering and the associated interferences. At the same time, it is well known that control of optical properties of matter by means of auxiliary quasiresonant electromagnetic fields is much more effective than by a static one. Electromagnetically-induced atomic coherence changes the optical properties of atomic samples in sometimes dramatic ways, and is responsible for such effects as population trapping, electromagnetically induced transparency (EIT), 'slow light', 'stopped light', to name a few [18–20].

*Corresponding author. Email: mhavey@odu.edu

ISSN 0950–0340 print/ISSN 1362–3044 online
© 2011 Taylor & Francis
DOI: 10.1080/09500340.2011.594180
http://www.informaworld.com

Downloaded by [Dmitriy Kupriyanov] at 10:27 07 October 2011

In this paper we are going to analyze how a resonant control field influences coherent backscattering of light. In particular, we consider CBS effects under conditions of electro-magnetically induced transparency. Our attention is focused on the spectral dependence of the relative amplitude of the backscattering cone in a steady-state regime, i.e. on the dependence of the enhancement factor on frequency of scattered light, which is assumed to be monochromatic. We show that a control field can essentially change the type of interference and even can cause destructive interference. For some scattering polarization channels and for some detunings of the probe light, the enhancement factor can be less than one. With the developed knowledge of the spectrum we also consider the dynamics of CBS in the case of pulsed probe radiation.

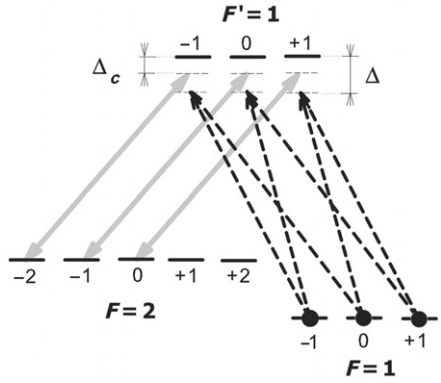

Figure 1. Excitation scheme for observation of the EIT effect in the system of hyperfine and Zeeman sublevels of the D_1-line of ^{87}Rb. The coupling field is applied with right-handed circular polarization to the $F=2 \rightarrow F'=1$ transition. The probe mode is applied to $F=1 \rightarrow F'=1$ transition and can cause different excitations depending on its polarization and propagation direction.

2. Basic assumptions

One of main quantitative characteristics of CBS is the enhancement factor, which determines the relative contribution of interference effects to the total scattered light intensity. In experiment, it is measured as the relative amount of light intensity scattered in a given direction inside the CBS cone compared with the background intensity registered outside the cone. In theory it is more convenient to evaluate the differential cross-section of scattering from the input to outgoing mode and calculate the enhancement factor as the ratio of this cross-section to its non-interfering part.

Our theoretical approach, allowing calculation of the differential cross-section of light scattered from optically thick ultracold atomic ensembles, is described in details in a series of papers [11,13–15]. This approach is based on a diagrammatic technique for non-equilibrium systems and allows us to obtain separately both interfering and non-interfering parts as a series over a number of incoherent scatterings.

The generalization of this approach to the case of the presence of a coherent control field was made in [21] and [22]. In Appendix 1, we show, as an example, the double scattering contributions to the differential cross-section. On the basis of these and similar expressions for higher order scattering contributions, we calculate here the spectral dependence of the enhancement factor. We consider probe light scattering from ultracold clouds of ^{87}Rb atoms, prepared in a magneto-optical trap after the trapping and repumping lasers and the quadrupole magnetic field are switched off. All atoms populate the F=1 hyperfine sublevel of the ground state, while the distribution over Zeeman sublevels is uniform. The spatial distribution of atoms is assumed to be spherically symmetric and Gaussian. For the typical conditions of the trap, the Doppler width is many times smaller than the natural line width of the excited state and the interatomic distances on average are much larger than the optical wavelength (dilute medium). This allows us to neglect all effects associated with atomic motion, and atomic collisions.

Probe radiation is quasi resonant with the $F=1 \rightarrow F'=1$ transition of the D_1 line (see Figure 1) and its polarization can be arbitrary. However, for definiteness we will consider right- or left-handed circularly polarized light. This light is assumed to be weak; all nonlinear effects connected with the probe radiation will be neglected. In our calculations, this field will be taken into account only in the first non-vanishing order. Besides the probe light, the atomic ensemble interacts with a coupling, control field. In this paper we will consider this field tuned to exact resonance with $F=2 \rightarrow F'=1$ transition. Its amplitude is determined by the Rabi frequency $\Omega_c = 2|V_{nm'}|$, $V_{nm'}$ are the transition matrix elements for the coupling mode between states $|n\rangle$ and $|m'\rangle \equiv |F, m'\rangle$, which we define with respect to the $|m'\rangle = |F=2, \quad m'=-1> \rightarrow |n\rangle = |F'=1, \quad n=0>$ hyperfine Zeeman transition. Other transition matrix elements are proportional to Ω_c and algebraic factors depending on corresponding Clebsch–Gordon coefficients.

The polarization of the control field is assumed to be right-handed and circular. The detuning of the probe laser frequencies from the corresponding atomic resonances is assumed to be much less than the hyperfine splitting. This circumstance, along with the relatively large hyperfine splitting in the excited state, allows us take into account only one hyperfine sublevel $F'=1$ of this state.

Downloaded by [Dmitriy Kupriyanov] at 10:27 07 October 2011

In this paper we will not focus our attention on the angular distribution and shape of the CBS cone, but will instead restrict ourselves by consideration of exact backscattering only. The ground state hyperfine splitting of ^{87}Rb is about 6.83 GHz, so Rayleigh and elastic Raman scattering (associated with the $F=1\to F'=1\to F=1$ transition) is well spectrally separated from inelastically Raman scattered light ($F=1\to F'=1\to F=2$). We will assume spectral selection under photo detection. The inelastic Raman component is assumed to be not registered. Depending on the type of polarization analyzer used for photo-detection, four main polarization schemes can be considered $H_+\to H_+$, $H_+\to H_-$, $H_-\to H_+$, $H_-\to H_-$. Here, $H_\pm$ represents the helicity of the input and outgoing light. Note that, despite homogeneous population of the Zeeman sublevels, the susceptibility tensor becomes essentially anisotropic due to the presence of the coupling field [21,22]. In such a case the enhancement factor depends not only on the relative polarizations of the input and output light but also on their specific types.

3. Results

The results of calculations of the spectrum of the enhancement factor for a weak control field are shown in Figure 2(*a*). The calculations were performed for an atomic cloud with a Gaussian radius equal to $r_0=0.5$ cm; maximal density is $n_0=3.2\cdot10^{10}\,\mathrm{cm}^{-3}$. The Rabi frequency of the control field is $\Omega_c=0.5\Gamma$. For a weak control field we observe a not particularly surprising behavior of the spectrum. Against a background typical for the spectral dependence of the CBS effect we see a narrow spectral gap that has its origin in the decreasing of the optical depth of the cloud caused by the EIT phenomena. Under the EIT effect the probability of higher-order scattering relatively decreases compared with single scattering and all interference effects that connect with multiple scattering are reduced. The width of the gap in the spectrum is about the width of the transparency window determined by the EIT phenomenon. We point out only that there is a certain difference in the width for different polarization channels caused by the above-mentioned optical anisotropy of the atomic ensemble. The situation changes dramatically when the control Rabi frequency becomes comparable to or larger than the spontaneous decay rate. In Figure 2(*b*), which is calculated for $\Omega_c=3\Gamma$, in addition to the more noticeable anisotropy, an essential transformation of the spectrum takes place. The range of the structure of this spectrum connects with the difference in the Autler–Townes splitting for different

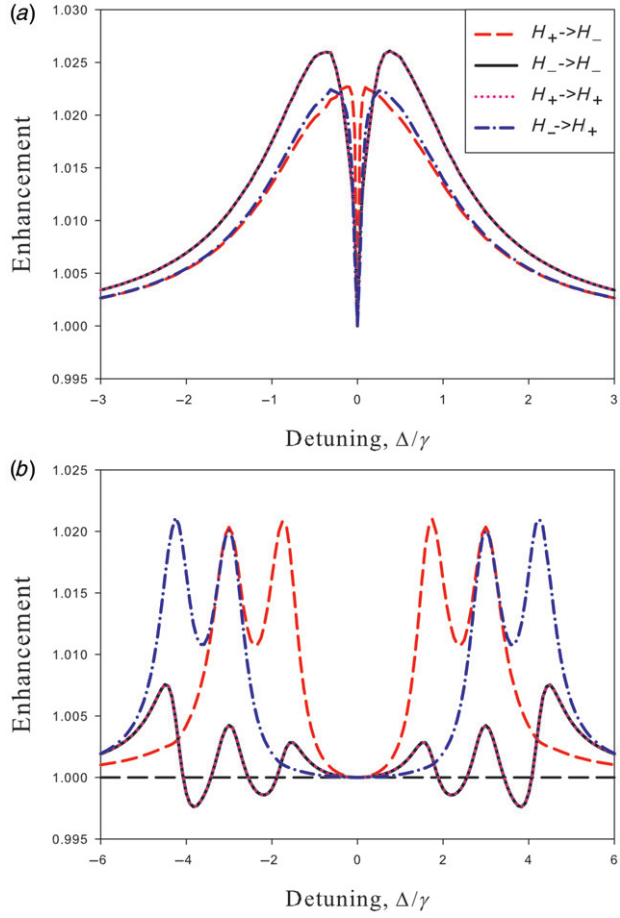

Figure 2. Spectrum of the enhancement factor (*a*) $\Omega_c=0.5\Gamma$, (*b*) $\Omega_c=3\Gamma$. (The color version of this figure is included in the online version of the journal.)

Zeeman transitions. The latter is caused by different dipole moments of the corresponding transitions and consequently with different Rabi frequencies for them. The maximal value of the enhancement factor for polarization channels with changing helicity is almost the same as for the weak control field, but for the case with preserving helicity we see qualitative modifications. The main one of these is that, instead of constructive interference for some spectral regions, we observe destructive interference. In these regions, for channels $H_-\to H_-$ and $H_+\to H_+$, the enhancement factor becomes less than unity. That is, in place of a CBS cone we have a CBS gap, or anticone. In spite of the relatively small value of the gap it seems physically important because CBS or weak localization itself in its 'traditional' interpretation connects with time-reversal and always causes enhancement in back scattering.

A similar effect for scattering of polarized electrons in a solid was shown in [23]. Following this, antilocalization in electron transport has been widely

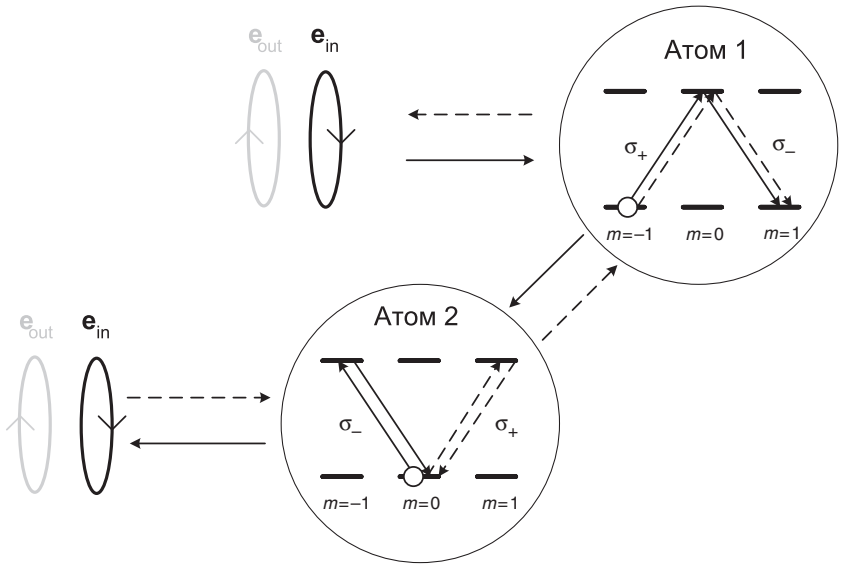

Figure 3. Diagram explaining the antilocalization phenomenon in the example of double scattering in the helicity preserving scattering channel. Only the interfering transitions initiated by the probe are shown and the presence of the control mode is specified in Figure 1.

Downloaded by [Dmitriy Kupriyanov] at 10:27 07 October 2011

studied in a range of physical systems where electrons interact directly with magnetic impurities and where the spin-orbit interaction is important [24,25]. The possibility to observe destructive interference in the case of light scattering from ultracold atomic ensemble was predicted for the first time in [13]. This effect was explained in [13] by the hyperfine interaction in atoms and by possible interference of transitions through different hyperfine sublevels of excited atomic states. In the case considered now, the mechanism of antilocalization is different. This is emphasized by Figure 2(*b*), in which the results are obtained for only one excited state sublevel $F' = 1$ without taking into account possible hyperfine interactions.

The fundamental possibility of destructive interference under multiple scattering connected with the coupling field is illustrated in Figure 3. Here, we show double backscattering of a positive helicity incoming photon from the probe light beam on a system consisting of two ^{87}Rb atoms; the exit channel consists of detection of light also of positive helicity. Here, the double scattering is a combination of the Raleigh-type and Raman-type transitions. In the direct path, the scattering consists of a sequence of Rayleigh-type scattering in the first step and of Raman-type scattering in the second one. In the reciprocal path, Raman-type scattering occurs first, and the positive helicity photon undergoes Rayleigh-type scattering in the second step. There is an important difference in the transition amplitudes associated with Raleigh process for these two interfering channels. Indeed, in the direct and reciprocal path the scattered mode is coupled with different Zeeman transitions. In the absence of a coupling field these transitions have the same amplitude and we always have constructive interference. The coupling field essentially modifies the scattering process and this modification is different for different Zeeman transitions. For definite frequencies of probe light, the scattering amplitudes connecting the direct and reciprocal scattering channels can be comparable in absolute value but can have phases shifted by an angle close to π. In this case, these two channels suppress each other. The considered example is not the only one, and appears only in the double scattering channel. There are some others that lead to constructive interference. In the higher scattering order the situation is similar. That is why in our results we have only partial destructive interference and for the considered parameters only a small suppression of backscattering.

Note that the antilocalization effect discussed in [13] takes place for essentially non-resonant light and consequently is difficult for observation, because it is challenging to prepare clouds with large optical depth for such radiation. The effect considered here takes place for radiation that is not far from resonance. It makes this case more promising for experimental verification. Note also that similar antilocalization phenomena can be observed in the case when the control field is absent but the probe radiation is strong enough to make the Autler–Townes splitting noticeable [26].

Consider now how these peculiarities in the spectrum manifest themselves in time-dependent CBS

Downloaded by [Dmitriy Kupriyanov] at 10:27 07 October 2011

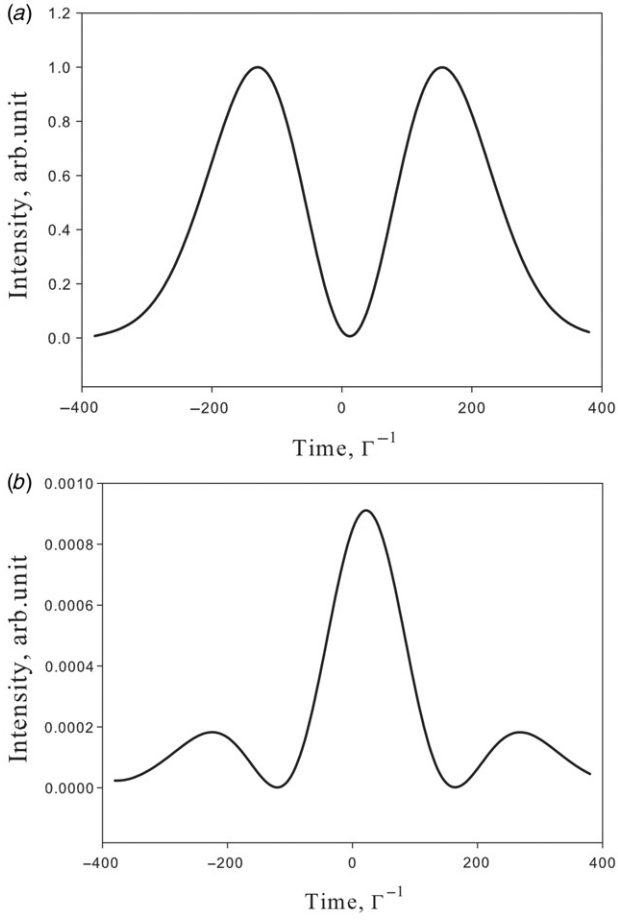

Figure 4. Shapes of the outgoing pulse (*a*) single scattering, (*b*) double scattering.

in the case of a pulsed probe light. Here, the most interesting effects are observed for a weak control field when peculiarities in the spectrum are sharp. Different spectral components of the input pulse scatter differently and it is the reason for the essential transformation of the spectrum and, consequently, the time profile of the pulse. Scattered light has a deficit of near resonant photons for which the EIT mechanism works best. The gap in the spectrum causes light beating effects, which are different for scattering of different orders. In Figure 4 we show shapes of pulses that undergo single (Figure 4(*a*)) and double (Figure 4(*b*)) scattering for the $H_+ \to H_-$ polarization channel. These graphs are calculated for a cloud with $n_0 = 3.2 \cdot 10^{10}\,\mathrm{cm}^{-3}$ and $r_0 = 0.5\,\mathrm{cm}$. The input pulse has a Gaussian shape $I = I_0 \exp(-t^2/\tau^2)$, the length of the pulse is $\tau = 200\Gamma^{-1}$.

The shapes of the single and doubly scattered pulses are essentially different. Most important is that the intensity peaks for them are separated in time. When single scattering intensity is maximal, double scattering is very small – and vice versa. This effect arises through the relative time scales associated with single scattering in comparison with double scattering. Figures 4 and 5 are built on the same timescale, so direct comparison shows that the enhancement pulse is many times narrower than the incident pulse or any of the peaks depicted in Figure 4(*a*) and (*b*), as illustrated in Figure 5. For comparison, the input pulse shape is also shown in Figure 5.

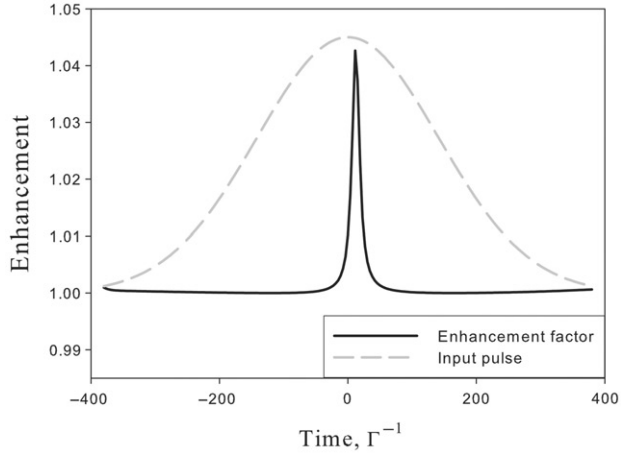

Figure 5. Time dependence of the enhancement factor in the case of pulsed probe radiation. Input pulse shape (in arbitrary intensity units) is shown in gray.

Acknowledgements

This work was supported by the Russian Foundation for Basic Research (Grant Nos. 08-02-91355 and 10-02-00103). M.H. acknowledges support from the National Science Foundation (NSF-PHY-0654226).

References

[1] Ishimaru, J.; Kuga, Y. *J. Opt. Soc. Am. A* **1984,** *1,* 809–813.
[2] Wolf, P.E.; Maret, G. *Phys. Rev. Lett.* **1985,** *55,* 2696–2699.
[3] Van Albada, M.P.; Lagendijk, A. *Phys. Rev. Lett.* **1985,** *55,* 2692–2695.
[4] Sheng, P., Ed. *Scattering and Localization of Classical waves in Random Media*; World Scientific: Singapore, 1990; p 648.
[5] Sheng, P. *Introduction to Wave Scattering, Localization, and Mesoscopic Phenomena*; Academic Press: San Diego, 1995; p 339.
[6] Kuz'min, V.L.; Romanov, V.P. *Phys. Usp.* **1996,** *39,* 231–260.
[7] Labeyrie, G.; de Tomasi, F.; Bernard, J.-C.; Müller, C.A.; Miniatura, C.; Kaiser, R. *Phys. Rev. Lett.* **1999,** *83,* 5266–5269.
[8] Labeyrie, G.; Müller, C.A.; Wiersma, D.S.; Miniatura, C.; Kaiser, R. *J. Opt. B: Quantum Semiclass. Opt.* **2000,** *2,* 672–685.

[9] Kulatunga, P.; Sukenik, C.I.; Balik, S.; Havey, M.D.; Kupriyanov, D.V.; Sokolov, I.M. *Phys. Rev. A* **2003,** *68,* 033816.
[10] Jonckheere, T.; Müller, C.A.; Kaiser, R., et al. *Phys. Rev. Lett.* **2000,** *85,* 4269–4272.
[11] Kupriyanov, D.V.; Sokolov, I.M.; Kulatunga, P.; Sukenik, C.I.; Havey, M.D. *Phys. Rev. A.* **2003,** *67,* 013814.
[12] Labeyrie, G.; Delande, D.; Müller, C.A.; Miniatura, C.; Kaiser, R. *Phys. Rev. A* **2003,** *67,* 033814.
[13] Kupriyanov, D.V.; Sokolov, I.M.; Havey, M.D. *Opt. Commun.* **2004,** *243,* 165–173.
[14] Datsyuk, V.M.; Sokolov, I.M. *JETP* **2005,** *102,* 724.
[15] Kupriyanov, D.V.; Sokolov, I.M.; Sukenik, C.I.; Havey, M.D. *Laser Phys. Lett.* **2006,** *3,* 223–243.
[16] Müller, C.A.; Miniatura, C.; Wilkowski, D.; Kaiser, R.; Delande, D. *Phys. Rev. A* **2005,** *72,* 053405.
[17] Sigwarth, O.; Labeyrie, G.; Jonckheere, T.; Delande, D.; Kaiser, R.; Miniatura, C. *Phys. Rev. Lett.* **2004,** *93,* 143906.
[18] Marangos, J.P. *J. Mod. Opt.* **1998,** *45,* 471–503.
[19] Lukin, M.D. *Rev. Mod. Phys.* **2003,** *75,* 457–472.
[20] Fleischhauer, M.; Imamoglu, A.; Marangos, J.P. *Rev. Mod. Phys.* **2005,** *77,* 633–673.
[21] Datsyuk, V.M.; Sokolov, I.M.; Kupriyanov, D.V.; Havey, M.D. *Phys. Rev. A* **2006,** *74,* 043812.
[22] Datsyuk, V.M.; Sokolov, I.M.; Kupriyanov, D.V.; Havey, M.D. *Phys. Rev. A* **2008,** *77,* 033823.
[23] Gorodnichev, E.E.; Dudarev, S.L.; Rogozkin, D.B. *Sov. Phys. JETP* **1990,** *70,* 853.
[24] Zumbäuhl, D.M.; Miller, J.B.; Marcus, C.M.; Campman, K.; Gossard, A.C. *Phys. Rev. Lett.* **2002,** *89,* 276803.
[25] Winkler, R. *Spin-orbit Coupling Effects in Two-dimensional Electron and Hole Systems*; Springer Tracts in Modern Physics 191; Springer-Verlag: Heidelberg, 2003.
[26] Shatokhin, V.; Wellens, T.; Grémaud, B.; Buchleitner, A. *Phys. Rev. A* **2007,** *76,* 043832.
[27] Varshalovich, D.A.; Maskalev, A.N.; Khersonskii, V.K. *Quantum Theory of Angular Momentum*; World Scientific: Singapore, 1988.

Downloaded by [Dmitriy Kupriyanov] at 10:27 07 October 2011

Appendix 1. The cross-section of the scattering process

The scattering process is typically described by the differential cross-section for light scattered into the solid angle Ω. If the system is dilute but optically dense than the total outcome can be expressed as the sum of the contributions of the subsequent scattering events, see [10–16]

$$\frac{\mathrm{d}\sigma}{\mathrm{d}\Omega}=\sum_{a=1}^{N}\frac{\mathrm{d}\sigma_a}{\mathrm{d}\Omega}+\sum_{a\neq b}\frac{\mathrm{d}\sigma_{ab}}{\mathrm{d}\Omega}+\sum_{a\neq b\neq c}\frac{\mathrm{d}\sigma_{abc}}{\mathrm{d}\Omega}+\cdots. \tag{1}$$

Through macroscopic-electrodynamics based self-consistent averaging in the dilute disordered system, this series is converging rapidly such that any events of possible recurrent scattering (when the atomic numerator gives $a=c$ etc) can be safely ignored. We consider as an example the calculation scheme in the second order, which can be straightforwardly generalised on the higher orders. For the specific scattering channel in the backward direction, the second-order contribution from two randomly selected atoms is given by the sum of two terms

$$\frac{\mathrm{d}\sigma_{12}}{\mathrm{d}\Omega}=\frac{\mathrm{d}\sigma_{12}^{(L)}}{\mathrm{d}\Omega}+\frac{\mathrm{d}\sigma_{12}^{(C)}}{\mathrm{d}\Omega} \tag{2}$$

where the first term is normally called a 'ladder' term describing the contribution of successive double scattering of a photon of frequency ω, wave vector $\mathbf{k}$, and polarization $\mathbf{e}$ to the outgoing mode ω', $\mathbf{k}'$, $\mathbf{e}'$ on atom $a=1$ first and atom $b=2$ second. A similar term contributes to the expansion (1) for the reciprocal path with $a=2$ and $b=1$. The second 'crossed' term is associated with interference between these scattering events. For the sake of clarity let us specify the polarization of the incoming photon by Cartesian unit vector $\mathbf{e}_\mu$ with $\mu=x,\ y$ ($\mathbf{k}\parallel z$) and of the outgoing photon by $\mathbf{e}'_\nu$ with $\nu=x',\ y'$ ($\mathbf{k}'\parallel z'$).

Then scattering in the particular polarization channel from $\mathbf{e}_\mu$ to $\mathbf{e}'_\nu$ is described by successive double scattering in the 'ladder' contribution and is given by

$$\begin{aligned}\frac{\mathrm{d}\sigma_{12}^{(L)}}{\mathrm{d}\Omega}=&\sum_{i,j,k,l}\sum_{\bar{i},\bar{j},\bar{k},\bar{l}}\frac{\omega_{12}^4}{c^4}\frac{\omega\omega'^3}{c^4}\frac{1}{r_{12}^2}\\&\times X_{\nu i}(\infty,\mathbf{r}_2,\omega')\alpha_{ik}^{m''_2m_2}(\omega_{12}-\mathbf{k}_{12}\mathbf{v}_2)X_{kl}(\mathbf{r}_2,\mathbf{r}_1,\omega_{12})\\&\times\alpha_{lj}^{m''_1m_1}(\omega-\mathbf{k}\mathbf{v}_1)X_{j\mu}(\mathbf{r}_1,\ -\infty,\omega)\\&\times\Big[X_{\nu\bar{i}}(\infty,\mathbf{r}_2,\omega')\alpha_{\bar{i}\bar{k}}^{m''_2m_2}(\omega_{12}-\mathbf{k}_{12}\mathbf{v}_2)X_{\bar{k}\bar{l}}(\mathbf{r}_2,\mathbf{r}_1,\omega_{12})\\&\times\alpha_{\bar{l}\bar{j}}^{m''_1m_1}(\omega-\mathbf{k}\mathbf{v}_1)X_{\bar{j}\mu}(\mathbf{r}_1,\ -\infty,\omega)\Big]^*\end{aligned} \tag{3}$$

where the photon's output and virtual intermediate frequency are affected by both the Raman and residual Doppler effects

$$\begin{aligned}\omega_{12}&=\omega-\omega_{m''_1m_1}+(\mathbf{k}_{12}-\mathbf{k})\mathbf{v}_1\\\omega'&=\omega_{12}-\omega_{m''_2m_2}+(\mathbf{k}'-\mathbf{k}_{12})\mathbf{v}_2\end{aligned} \tag{4}$$

where the following notation is used: $\mathbf{v}_1$ and $\mathbf{v}_2$ are the velocities of the first and the second atoms; $\mathbf{k}_{12}$ and $\mathbf{k}'$ are the photon's wave vectors in the intermediate and outgoing modes; $r_{12}=|\mathbf{r}_2-\mathbf{r}_1|$ is the relative distance between the atoms. For the intermediate mode the wave vector is given by $\mathbf{k}_{12}=(\omega_{12}/c)(\mathbf{r}_2-\mathbf{r}_1)/|\mathbf{r}_2-\mathbf{r}_1|$.

There are several important ingredients contributing to the cross-section. The first is the scattering tensor, which is given by

$$\begin{aligned}\alpha_{lj}^{(m''m)}(\Delta)=&-\sum_{m'(n),n}\frac{1}{\hbar}\frac{(d_l)_{m''n}(d_j)_{nm}}{\Delta+i\Gamma/2}\\&\times\left\{1-\frac{|V_{nm'}|^2}{\Delta+i\Gamma/2}\frac{1}{\Delta_c-\Delta+\Sigma_{nm'}(\Delta)}\right\}.\end{aligned} \tag{5}$$

With reference to Figure 1 the self-energy radiation term $\Sigma_{nm'}(\Delta)=|V_{nm'}|^2/(\Delta+i\Gamma/2)$ is expressed by transition matrix elements $V_{nm'}$ for the control mode coupling the non-populated states $|n\rangle$ and $|m'\rangle\equiv|F,\ m'\rangle$ the frequency detunings Δ and Δ_c are respectively the offsets of the probe ω

Downloaded by [Dmitriy Kupriyanov] at 10:27 07 October 2011

and control ω_c from the resonance $\Delta = \omega - \omega_{F'F}$ ($F=1$) and $\Delta_c = \omega_c - \omega_{F'F}$ ($F=2$); Γ is the natural radiation rate of the excited states; $(d_j)_{nm}$ represents the dipole transition moments between the lower $|m\rangle \equiv |F, m\rangle$ and upper $|n\rangle \equiv |F', n\rangle$ states. The scattering tensor determines the amplitude of the single scattering event for either the elastic or inelastic channel accompanied by the atomic transition from the state $|m\rangle \equiv |F, m\rangle$ with $F=1$ to the state $|m''\rangle \equiv |F, m''\rangle$ with $F=1$ (Rayleigh channel) or $F=2$ (inelastic Raman channel), see Figure 1.

Before, between, and after two successive scattering events the photon propagates in the bulk medium in accordance with the macroscopic Maxwell theory. The transformation of its amplitude is relevantly described by the formalism of the Green's propagation function, see [15,21,22]. The matrix functions $X_{kl}(\mathbf{r}_2, \mathbf{r}_1; \omega)$ perform the slowly varying amplitudes associated with the photon-retarded-type Green's function. They follow the transformation of the light amplitude and polarization between points $\mathbf{r}_1$ and $\mathbf{r}_2$. One of these points can approach infinity for either the input or output scattering channels. The subscript tensor indices k and l are always associated with the specific frame where the propagation direction $\mathbf{r}_2 - \mathbf{r}_1$ is associated with the z-axis. The components k and l belong to the orthogonal plane z and we enumerate them by 1 (x-axis) and 2 (y-axis). In this basis, the Green's function slowly varying components can be expressed as follows

$$\begin{aligned}
X_{11}(\mathbf{r}_2, \mathbf{r}_1; \omega) &= e^{i\phi_0(\mathbf{r}_2, \mathbf{r}_1)}(\cos\phi(\mathbf{r}_2, \mathbf{r}_1) - i\sin\phi(\mathbf{r}_2, \mathbf{r}_1)n_x)\\
X_{22}(\mathbf{r}_2, \mathbf{r}_1; \omega) &= e^{i\phi_0(\mathbf{r}_2, \mathbf{r}_1)}(\cos\phi(\mathbf{r}_2, \mathbf{r}_1) + i\sin\phi(\mathbf{r}_2, \mathbf{r}_1)n_x)\\
X_{12}(\mathbf{r}_2, \mathbf{r}_1; \omega) &= ie^{i\phi_0(\mathbf{r}_2, \mathbf{r}_1)}\sin\phi(\mathbf{r}_2, \mathbf{r}_1)\big(n_y + in_z\big)\\
X_{21}(\mathbf{r}_2, \mathbf{r}_1; \omega) &= ie^{i\phi_0(\mathbf{r}_2, \mathbf{r}_1)}\sin\phi(\mathbf{r}_2, \mathbf{r}_1)\big(n_y - in_z\big)
\end{aligned} \tag{6}$$

where

$$\begin{aligned}
\phi_0(\mathbf{r}_2, \mathbf{r}_1) &= \frac{2\pi\omega}{c}\int_{\mathbf{r}_1}^{\mathbf{r}_2}\chi_0(\mathbf{r}, \omega)\mathrm{d}s;\\
\phi(\mathbf{r}_2, \mathbf{r}_1) &= \frac{2\pi\omega}{c}\int_{\mathbf{r}_1}^{\mathbf{r}_2}\chi(\mathbf{r}, \omega)\mathrm{d}s
\end{aligned} \tag{7}$$

performs the phase integrals along the path s linking the points $\mathbf{r}_1$ and $\mathbf{r}_2$ such that $\mathbf{r} = \mathbf{r}(s)$ in the integrand. The parameters of these integrals are expressed by components of the dielectric susceptibility tensor of the medium.

Because of the specific symmetry of the problem, see Figure 1 it is convenient to define these integrals in the alternative basis set of circular polarizations. It can be defined by the following expansion $\mathbf{e}_0 = \mathbf{e}_z$, $\mathbf{e}_{\pm1} = \mp(\mathbf{e}_x \pm \mathbf{e}_y)/\sqrt{2}$ in the Cartesian frame and it requires co/contravariant notation in writing the tensors products, see [27]. The spectrally dependent parameters $\chi(\mathbf{r}, \omega)$, $\chi_0(\mathbf{r}, \omega)$ and symbolic vector $\overrightarrow{\chi}(\mathbf{r}, \omega)$ perform the expansion coefficients of the susceptibility tensor projected on the plane orthogonal to $\mathbf{r}_2 - \mathbf{r}_1$ in the basis set of the Pauli matrices $\overrightarrow{\sigma} = (\sigma_x, \sigma_y, \sigma_z)$. This tensor projection thus can be written

$$\tilde{\chi}_q{}^{q'}(\mathbf{r}, \omega) = \chi_0(\mathbf{r}, \omega)\delta_q{}^{q'} + \big(\overrightarrow{\chi}(\mathbf{r}, \omega)\cdot\overrightarrow{\sigma}\big)_q{}^{q'} \tag{8}$$

where q, $q' = \pm1$. To find the parameters of the phase integrals the components $\tilde{\chi}_q{}^{q'}$ on the left-hand side of the expansion (8) should be explicitly expressed by the components of the susceptibility tensor in the laboratory frame $\chi_q{}^{q'}$. Then $\chi(\mathbf{r}, \omega)$ is the complex length of vector $\overrightarrow{\chi}(\mathbf{r}, \omega)$ and $\overrightarrow{n}(\omega)$ is its 'director' , which are given by

$$\begin{aligned}
\chi^2(\mathbf{r}, \omega) &= \chi_x^2(\mathbf{r}, \omega) + \chi_y^2(\mathbf{r}, \omega) + \chi_z^2(\mathbf{r}, \omega)\\
\overrightarrow{n} &= \overrightarrow{n}(\omega) = \overrightarrow{\chi}(\mathbf{r}, \omega)/\chi(\mathbf{r}, \omega).
\end{aligned} \tag{9}$$

We additionally assume that the atomic polarization is homogeneous along the atomic sample such that the 'director' $\overrightarrow{n}(\omega)$ is constant along the path in the phase integrals' representation of Green's function (6).

The local reference frame is linked with the laboratory frame via a rotational transformation characterized by Euler angles α, β, γ. Then the susceptibility tensor components projected onto the plane orthogonal to the light ray direction and defined in the basis of circular polarizations, are given by

$$\begin{aligned}
\tilde{\chi}_{+1}{}^{+1}(\ldots) &= \frac{(1+\cos\beta)^2}{4}\chi_{+1}^{+1}(\ldots) + \frac{(1-\cos\beta)^2}{4}\chi_{-1}^{-1}(\ldots)\\
&\quad + \frac{\sin^2\beta}{2}\chi_0^0(\ldots),\\
\tilde{\chi}_{-1}{}^{-1}(\ldots) &= \frac{(1-\cos\beta)^2}{4}\chi_{+1}^{+1}(\ldots) + \frac{(1+\cos\beta)^2}{4}\chi_{-1}^{-1}(\ldots)\\
&\quad + \frac{\sin^2\beta}{2}\chi_0^0(\ldots),\\
\tilde{\chi}_{-1}{}^{+1}(\ldots) &= \frac{1}{4}\mathrm{e}^{2\mathrm{i}\gamma}\sin^2\beta\big[\chi_{+1}^{+1}(\ldots) + \chi_{-1}^{-1}(\ldots) - 2\chi_0^0(\ldots)\big]\\
\tilde{\chi}_{+1}{}^{-1}(\ldots) &= \frac{1}{4}\mathrm{e}^{-2\mathrm{i}\gamma}\sin^2\beta\big[\chi_{+1}^{+1}(\ldots) + \chi_{-1}^{-1}(\ldots) - 2\chi_0^0(\ldots)\big]
\end{aligned} \tag{10}$$

where on the right-hand side the tensor components $\chi_q^{q'}(\ldots)$ are associated with the laboratory frame. On the basis of complex polarizations $\mathbf{e}_0$, $\mathbf{e}_{\pm1}$ this tensor has a symmetric diagonal structure and its components are given by

$$\begin{aligned}
\chi_q^{q'}(\mathbf{r}, \Delta) = -\delta_q^{q'}\frac{n_0(\mathbf{r})}{2F+1}\sum_{n(m), m'(m), m}\frac{1}{\hbar}\frac{|(\mathbf{d}\mathbf{e}_q^*)_{nm}|^2}{\Delta + i\Gamma/2}\\
\times\left\{1 - \frac{|V_{nm'}|^2}{\Delta + i\Gamma/2}\frac{1}{\Delta_c - \Delta + \Sigma_{nm'}(\Delta)}\right\}
\end{aligned} \tag{11}$$

where $n_0(\mathbf{r})$ is the local density of atoms and the states $|n\rangle$ and $|m'\rangle$ in the sum are unique for each $|m\rangle$ such that $n = n(m)$ and $m' = m'(m)$.

The 'crossed' term contribution in the differential cross-section (2) is expressed similarly to the 'ladder' term

$$\begin{aligned}
\frac{\mathrm{d}\sigma_{12}^{(C)}}{d\Omega} = \sum_{i,j,k,l}\sum_{\bar{i},\bar{j},\bar{k},\bar{l}}\frac{\omega_{12}^2}{c^2}\frac{\omega_{21}^2}{c^2}\frac{\omega\omega'^3}{c^4}\\
\times\frac{1}{r_{12}^2}\exp\left[i(\mathbf{k}+\mathbf{k}')(\mathbf{r}_1 - \mathbf{r}_2) + i\frac{(\omega_{12} - \omega_{21})}{c}r_{12}\right]\\
\times X_{vi}(\infty, \mathbf{r}_2, \omega')\alpha_{ik}^{m_2''m_2}(\omega_{12} - \mathbf{k}_{12}\mathbf{v}_2)X_{kl}(\mathbf{r}_2, \mathbf{r}_1, \omega_{12})\\
\times\alpha_{lj}^{m_1''m_1}(\omega - \mathbf{k}\mathbf{v}_1)X_{j\mu}(\mathbf{r}_1, -\infty, \omega)\\
\times\left[X_{v\bar{i}}(\infty, \mathbf{r}_1, \omega')\alpha_{\bar{i}\bar{k}}^{m_1''m_1}(\omega_{21} - \mathbf{k}_{21}\mathbf{v}_1)X_{\bar{k}\bar{l}}(\mathbf{r}_1, \mathbf{r}_2, \omega_{21})\right.\\
\left.\times\alpha_{\bar{l}j}^{m_2''m_2}(\omega - \mathbf{k}\mathbf{v}_2)X_{j\mu}(\mathbf{r}_2, -\infty, \omega)\right]^*
\end{aligned} \tag{12}$$

where for the reciprocal path the frequency ω_{21} given by

$$\omega_{21} = \omega - \omega_{m_2'' m_2} + (\mathbf{k}_{21} - \mathbf{k})\mathbf{v}_2 \tag{13}$$

is different from ω_{12} but ω' for the scattering in the backward direction is the same.

In the macroscopic and disordered atomic system the 'crossed' term (12) contributes mainly in the narrow solid angle near backward direction ($\mathbf{k}' \approx -\mathbf{k}$). For any other directions this term makes a negligible contribution. In higher orders of multiple scattering the 'ladder' and interference 'crossed' parts have a similar structure. All these term can be subsequently (moving from lower to higher orders) involved in the Monte Carlo simulation scheme. The cross-section should be averaged with the atomic density matrix over the initial states m_1, m_2,... and over the atomic velocity distribution for $\mathbf{v}_1$, $\mathbf{v}_2$.... This averaging is equivalent to the smoothed sum in the original expansion of the cross-section given by Equation (1).

Downloaded by [Dmitriy Kupriyanov] at 10:27 07 October 2011